J|A|C|S
ARTICLES
Published on Web 03/01/2005

Ionization Potentials of Fluoroindoles and the Origin of Nonexponential Tryptophan Fluorescence Decay in Proteins[⊥]

Tiqing Liu,[†] Patrik R. Callis,*[,†] Ben H. Hesp,[§] Mattijs de Groot,[||] Wybren Jan Buma,[||] and Jaap Broos*[,‡]

Contribution from the Department of Chemistry and Biochemistry, Montana State University, Bozeman, Montana 59717, Department of Biochemistry and Groningen Biomolecular Science and Biotechnology Institute (GBB), and Material Sciences Centre, Ultrafast Laser and Spectroscopy Laboratory, University of Groningen, Nijenborgh 4, 9747 AG Groningen, The Netherlands, and Van't Hoff Institute for Molecular Sciences, University of Amsterdam, Nieuwe Achtergracht 166, 1018 WV Amsterdam, The Netherlands

Received November 13, 2004; E-mail: pcallis@montana.edu; j.broos@chem.rug.nl

Abstract: This work reports an explanation for the unusual monoexponential fluorescence decay of 5-fluorotryptophan (5FTrp) in single-Trp mutant proteins [Broos, J.; Maddalena, F.; Hesp, B. H. *J. Am. Chem. Soc.* **2004**, *126*, 22−23] and substantially clarifies the origin of the ubiquitous nonexponential fluorescence decay of tryptophan in proteins. Our results strongly suggest that the extent of nonexponential fluorescence decay is governed primarily by the efficiency of electron transfer (ET) quenching by a nearby amide group in the peptide bond. Fluoro substitution increases the ionization potential (IP) of indole, thereby suppressing the ET rate, leading to a longer average lifetime and therefore a more homogeneous decay. We report experimental IPs for a number of substituted indoles including 5-fluoroindole, 5-fluoro-3-methylindole, and 6-fluoroindole, along with accurate ab initio calculations of the IPs for these and 20 related molecules. The results predict the IP of 5-fluorotryptophan to be 0.19 eV higher than that of tryptophan. 5-Fluoro substitution does not measurably alter the excitation-induced change in permanent dipole moment nor does it change the fluorescent state from ^1L_a to ^1L_b. In combination with electronic structure information this argues that the increased IP and the decreased excitation energy of the ^1L_a state, together 0.3 eV, are solely responsible for the strong reduction of electron transfer quenching. 6-Fluoro substitution is predicted to increase the IP by a mere 0.09 eV. In agreement with our conclusions, the fluorescence decay curves of 6-fluorotryptophan-containing proteins are well fit using only two decay times compared to three required for Trp.

Introduction

Tryptophan (Trp) fluorescence lifetimes and quantum yields in proteins are highly sensitive to environment. This sensitivity is widely exploited for the study of protein structural changes associated with folding/unfolding, ligand binding, and protein recognition.[1−5] Such sensitivity, however, appears to carry with it a price: Trp fluorescence in proteins almost always decays nonexponentially. Nonexponential decay considerably compromises effective use of fluorescence as a probe for properties that would induce nonexponential decay, e.g., rotational diffusion and resonance energy transfer. No consensus exists as to the cause of the nonexponential decay. Opinions are divided between the view that discrete subpopulations (most often assigned to different Trp χ_1 and χ_2 rotamers[6−10]) exhibit different decay times and, at the other extreme, the view that the excited population is homogeneous but has a time-dependent fluorescence spectrum that shifts to longer wavelengths on a nanosecond time scale.[11] Other more general views have also been expressed.[12−14] Other than a few exceptions due to histidine

[†] Montana State University.
[‡] Department of Biochemistry and Groningen Biomolecular Science and Biotechnology Institute (GBB), University of Groningen.
[§] Material Sciences Centre, University of Groningen.
[||] University f Amsterdam.
[⊥] Abbreviations: EII[mtl], the mannitol-specific transporting and phosphorylating enzyme from *E. coli*; Trp, tryptophan; 5FTrp, 5-fluorotryptophan; 6FTrp, 6-fluorotryptophan; NATA, *N*-acetyl-L-tryptophanamide; 5FNATA, *N*-acetyl-DL-5-fluorotryptophanamide; 3MI, 3-methylindole; 5FI, 5-fluoroindole; 5F3MI, 5-fluoro-3-methylindole; PG, 1,2-propylene glycol; ET, electron transfer; A_0, intrinsic anisotropy; IP, ionization potential; CT, charge transfer.

(1) Beechem, J. M.; Brand, L. *Annu. Rev. Biochem.* **1985**, *54*, 43−71.
(2) Eftink, M. R. *Methods Biochem. Anal.* **1991**, *35*, 127−205.
(3) Lakowicz, J. *Principles of Fluorescence Spectroscopy*, 2nd ed.; Plenum: 1999.
(4) Smirnov, A. V.; English, D. S.; Rich, R. L.; Lane, J.; Teyton, L.; Schwabacher, A. W.; Luo, S.; Thornburg, R. W.; Petrich, J. W. *J. Phys. Chem. B* **1997**, *101* (15), 2758−2769.
(5) Prendergast, F. G. *Curr. Opin. Struct. Biol.* **1991**, *1*, 1054−1059.
(6) Privat, J.-P.; Wahl, P.; Auchet, J.-C. *Biophys. Chem.* **1979**, *9*, 223−233.
(7) Petrich, J. W.; Chang, M. C.; McDonald, D. B.; Fleming, G. R. *J. Am. Chem. Soc.* **1983**, *105*, 3824−3832.
(8) Dahms, T. E. S.; Willis, K. J.; Szabo, A. G. *J. Am. Chem. Soc.* **1995**, *117*, 2321−2326.
(9) Hellings, M.; DeMaeyer, M.; Verheyden, S.; Hao, Q.; VanDamme, E. J. M.; Peumans, W. J.; Engelborghs, Y. *Biophys. J.* **2003**, *85*, 1894−1902.
(10) Ross, J. B. A.; Wyssbrod, H. R.; Porter, R. A.; Schwartz, G. P.; Michaels, C. A.; Laws, W. R. *Biochemistry* **1992**, *31* (6), 1585−1594.
(11) Lakowicz, J. *Photochem. Photobiol.* **2000**, *72*, 421−437.
(12) Bajzer, Z.; Prendergast, F. G. *Biophys. J.* **1993**, *65*, 2313−2323.
(13) Hudson, B. S.; Huston, J. M.; Soto-Campos, G. *J. Phys. Chem. A* **1999**, *103*, 2227−2234.
(14) Wlodarczyk, J.; Kierdaszuk, B. *Biophys. J.* **2003**, *85* (1), 589−598.

10.1021/ja043154d CCC: $30.25

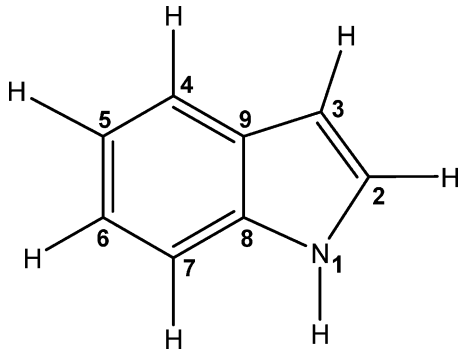

Figure 1. Structure of indole showing numbering convention.

cation[15] and disulfide quenching,[16] the intrinsic quenching of Trp fluorescence in proteins has long been thought to be caused by photoinduced electron transfer (ET) in which an electron is transferred from the indole ring to a nearby amide of the peptide backbone.[17−22] Recent QM−MM simulations show that electron transfer to the somewhat unlikely electron acceptor amide can be sensitively controlled by the electric field strength and direction caused by local charged and polar groups.[23,24]

Very recently Broos et al.[25] reported that the fluorescence decay of 5-fluorotryptophan (5FTrp) incorporated into single-Trp mutants of the mannitol transporter protein of E. coli, EII^{mtl}, is almost always *monoexponential*, even though the corresponding unmodified single Trp proteins show quite nonexponential decays.[26] By comparing the quantum yields and lifetimes of 3-methylindole (3MI) and *N*-acetyltryptophanamide (NATA)[27] to those of 5-fluoro-3-methylindole (5F3MI) and 5-fluoroNATA (5FNATA), they found that the amide side chains reduce the quantum yield relative to 5F3MI by only 17%, in contrast to the corresponding nonfluorinated molecule, where the amides reduce the yield by nearly 60%. The proposal was made that 5-fluoro substitution greatly inhibits electron transfer (ET) quenching.[25]

In considering possible mechanisms for how 5-fluoro substitution could effectively remove the lifetime heterogeneity, we note that elimination of ET quenching is reasonable, based on the discrete conformation model. ET rates are known to be extremely sensitive to the distance between donor and acceptor and to the local electrostatic microenvironment, because both affect the energy difference between the fluorescing and charge transfer (CT) state, and the coupling is dependent on distance and orientation. If 5-fluoro substitution affects the coupling and/or the energy difference, this would lend credence to the discrete conformation model.

On the other hand, if relaxation of the fluorescence spectrum during the excited-state lifetime of Trp is responsible for the nonexponential decay, this could be possible if the 5-fluoro substitution reduced the excitation-induced permanent dipole change (wavelength sensitivity to microenvironment), thereby removing the driving force for the relaxation.

In this paper, we investigate the proposition that ET, and with it lifetime heterogeneity, is effectively eliminated in 5FTrp, because fluoro substitution significantly raises the energy required to remove an electron from the indole ring; i.e., it raises the ionization potential (IP). An increased IP translates to a more positive Gibbs free energy change (ΔG_0) for ET as established by Rehm and Weller.[28] The weak electron accepting power of amides means that increasing ΔG_0 will substantially decrease the ET rate. We have carried out accurate ab initio calculations and measurements that predict the IP of 5FTrp to be 0.19 eV higher than that of Trp and the IP of 6FTrp to be 0.09 eV higher than that of Trp. We have also examined the solvent dependence of the fluorescence spectra for these and the fluorescence anisotropy spectra for 5FNATA, both of which help determine that the nature of the emitting state is virtually unchanged by the fluoro substitution. Below, we report these results and their ramifications.

Methods

Materials. D,L-5-FluoroTrp (5FTrp), D,L-6-fluoroTrp (6FTrp), and *N*-acetyl-L-tryptophanamide (NATA) were from Sigma; 5-fluoroindole (5-FI), 1-methylindole, 5-methylindole, and *p*-terphenyl were from Aldrich; 3-methylindole was from Fluka; and 6-fluoroindole (6FI) and 1,2-propylene glycol (PG) were from Across Organics. $C_{10}E_5$ detergent was from Kwant High Vacuum Oil Recycling and Synthesis, Bedum, The Netherlands. Fluorescent impurities were removed as described.[29]

Biosynthetic incorporation of tryptophan analogues in EII^{mtl} and purification of the proteins were performed as described in detail elsewhere.[30] The incorporation of Trp analogues instead of Trp had no measurable effect on the mannitol binding affinity and mannitol phosphorylation activity.

Synthesis. NMR spectra were recorded on a Varian Gemini-200 (^{1}H NMR at 200 MHz, ^{13}C NMR at 50.3 MHz). Mass spectrometry (electron impact) was performed with a JEOL JMS-600H.

5FNATA: The synthesis was performed, starting with D,L-5FTrp, as described for NATA.[31] ^{1}H NMR (CD_3OD): δ 2.0 (s, 3H), 3.0−3.3 (d-AB, 2H), 4.6 (t, 1H), 6.8−6.9 (t, 1H), 7.2−7.3 (m, 3H). ^{13}C NMR (CD_3OD): δ 19.6 (CH_3), 26.1 (C_β), 52.3 (C_α), 101.1 (C-4), 107.5 (C-6), 108.4 (C-3), 110.0 (C-7), 123.5 (C-2), 131.6 (C-9), 136.2 (C-8), 156.0 (C-5), 170.2 (NCO), 173.8 ($CONH_2$). MS *m*/*z*: 263 (M^+), 204 (($M^+ - CONH_2-CH_3$), 148 (5F-3-methyleneindolium).

5F3MI: 5-fluoro-3-carboxaldehyde was synthesized as described.[32] The product was purified via SiO_2 column chromatography with cyclohexane/ethyl acetate (1:1) as mobile phase. After evaporation of the solvent and drying under vacuum/P_2O_5, the product was reduced with $LiAlH_4$ to 5F3MI as described for 5-bromoindole-3-carboxyal-

(15) De-Beuckeleer, K.; Volckaert, G.; Engelborghs, Y. *Proteins* **1999**, *36*, 42−53.
(16) Weisenborn, P. C. M.; Meder, H.; Egmond, M. R.; Visser, T. J. W. G.; van Hoek, A. *Biophys. Chem.* **1996**, *58*, 281−288.
(17) Cowgill, R. W. *Arch. Biochem. Biophys.* **1963**, *100*, 36−44.
(18) Petrich, J. W.; Chang, M. C.; Fleming, G. R. *NATO ASI Ser.* **1985**, *85*, 77−80.
(19) Ricci, R. W.; Nesta, J. M. *J. Phys. Chem.* **1976**, *80*, 974−980.
(20) Chen, Y.; Liu, B.; Yu, H.-T.; Barkley, M. D. *J. Am. Chem. Soc.* **1996**, *118*, 9271−9278.
(21) Chen, Y.; Barkley, M. D. *Biochemistry* **1998**, *37*, 9976−9982.
(22) Ababou, A.; Bombarda, E. *Protein Sci.* **2001**, *10*, 2102−2113.
(23) Callis, P. R.; Vivian, J. T. *Chem. Phys. Lett.* **2003**, *369*, 409−414.
(24) Callis, P. R.; Liu, T. *J. Phys. Chem. B* **2004**, *108*, 4248−4259.
(25) Broos, J.; Maddalena, F.; Hesp, B. H. *J. Am. Chem. Soc.* **2004**, *126*, 22−23.
(26) Dijkstra, D. S.; Broos, J.; Visser, A. J. W. G.; vanHoek, A.; Robillard, G. T. *Biochemistry* **1997**, *36* (16), 4860−4866.
(27) 3MI and NATA are useful model compounds. NATA has two amides connected to the indole ring just as in the protein and does not have the ammonium and carboxylate characteristic of the free amino acid Trp at pH 7. The amides are separated from the system of the indole ring by two saturated carbons. Therefore, 3MI has very nearly the same electronic properties, without the possibility of electron transfer to the amides.
(28) Rehm, D.; Weller, A. *Isr. J. Chem.* **1970**, *8*, 259−271.
(29) Dijkstra, D. S.; Broos, J.; Robillard, G. T. *Anal. Biochem.* **1996**, *240* (1), 142−147.
(30) Broos, J.; Gabellieri, E.; Biemans-Oldehinkel, E.; Strambini, G. B. *Protein Sci.* **2003**, *12* (9), 1991−2000.
(31) Holst, P. B.; Anthoni, U.; Christophersen, C.; Larsen, S.; Nielsen, P. H.; Puschl, A. *Adv. Chem. Phys.* **1998**, *52* (6), 683−693.
(32) Mor, M.; Rivara, S.; Silva, C.; Bordi, F.; Plazzi, P. V.; Spadoni, G.; Diamantini, G.; Balsamini, C.; Tarzia, G.; Fraschini, F.; Lucini, V.; Nonno, R.; Stankov, B. M. *J. Med. Chem.* **1998**, *41* (20), 3831−3844.

dehyde.[33] The product was twice crystallized from Pet ether 60−80 and further purified by SiO_2 column chromatography (cyclohexane/ethyl acetate (1/1)). White crystals were obtained after sublimation of the product under vacuum at 35 °C. ^{1}H NMR ($CDCl_3$): δ 2.3 (s, 3H), 6.9−7.0 (m, 2H), 7.2−7.3 (m, 2H). ^{13}C NMR ($CDCl_3$): δ 9.4 (CH_3), 103.6 (C-4), 110.0 (C-6), 111.6 (C-7), 111.8 (C-3), 123.3 (C-2), 128.5 (C-9), 132.6 (C-8), 157.6 (C-5). MS *m*/*z*: 148 (M^+).

Computations. Gaussian98[34] was used for all ground and radical cation calculations in the determination of ionization potentials. Geometry optimizations were carried out with density functional theory (DFT) calculations at the B3LYP/6-31G* level, where B3LYP denotes the Becke3−Lee−Yang−Parr hybrid functional, B3LYP.[35] Single-point calculations were carried out using the same method and also using B3LYP/6-311+G(2df,2p), which has been found to provide good agreement with experiment.[36] Zero-point vibrational energy corrections were made using the 6-31G* basis without frequency scaling.

The Molcas5.4[37] package was used for CASPT2 calculations, using an atomic natural orbital (ANO) type basis set[37,38] contracted to C, N, O 3s2p1d/H 2s, with an active space of 9 valence π MOs and 10 active electrons. For the indole−amide systems, the active space included at least 3 indole π MOs and at most 2 amide π MOs. The CASSCF calculations used state averaging, with the number of roots varying from 8 to 50, depending on the geometry of the system.

INDO/S2-CIS (ZINDO)[39] calculations used Mataga−Nishimoto[39,40] electron repulsion parameters in conjunction with interaction scaling factors $f_\sigma = 1.267$ and $f_\pi = 0.585$ and INDO2. The configuration interaction included 196 singly excited configurations generated from the 14 highest filled MOs and the lowest empty MOs, with no energy selection. The S2 designation signifies use of the improved set of parameters for oxygen suggested by Li et al.[41]

A. Identification of States. Identification of the quasi degenerate ^1L_a and ^1L_b states is most reliably done by examination of transition densities,[42] but in this work ^1L_a is clearly identified by its larger transition dipole and larger permanent dipole relative to ^1L_b. The CT state of interest here is largely composed of a single configuration wherein one electron is promoted from the highest occupied π MO (HOMO) of the indole ring to the lowest unoccupied π^* MO (LUMO) of the amide.

Spectroscopy and Lifetimes. Absorption spectra were recorded with a Cary 100UV/VIS spectrophotometer. The high absorption of DMF for wavelengths below 280 nm prevented accurate determination of the absorption of 5FNATA and NATA at these wavelengths. The emission spectra of model compounds and the excitation anisotropy spectra were recorded on a Fluorolog3-22 fluorospectrometer (Jovin Yvon) equipped with Glan-Thompson polarizers in L-format. Excitation and emission monochromators were calibrated following instructions from the manufacturer. Excitation was at 293 nm, and bandwidths of 2 and 5 nm were employed for excitation and emission, respectively. Emission spectra were corrected for solvent and instrument response. For the excitation anisotropy measurements, a liquid N_2 cryostat (Oxford Instruments Ltd, model DN1714) was used to cool the sample to −55 °C. These samples were prepared by mixing the fluorophore in 50 mM phosphate buffer pH 7.5 with PG (10:90 (v/v)) and were subsequently transferred to a 5 mm × 5 mm cuvette. The final fluorophore concentration was 20−30 μM. The reproducibility of anisotropy values was found to be ±0.01. The spectra at low temperature were recorded with the polarizers in magic angle configuration, and spectra were corrected for instrument response. The excitation and emission band-passes were set at 2 and 5 nm, respectively.

Fluorescence spectra of the 5FTrp-containing mutants were recorded on a SLM-Aminco SPF-500 fluorometer at room temperature. Excitation was at 297 nm with excitation and emission band-passes at 2 and 5 nm, respectively. All spectra were corrected for fluorescence from the buffer and for instrument response.

Fluorescence lifetime (TCSPC) measurements were performed using a frequency-tripled modelocked Ti:Sapphire laser system for excitation (Coherent Inc: VERDI-5W, MIRA-900-F, Pulse Picker 9200, Harmonics Generator 9200), delivering subpicosecond pulses of approximately 5 pJ at a 1.9 MHz repetition rate. The fluorescence was collected at 90° via an f/2 collimating lens, a HNP'B near UV polarizer (3M), and a 368 nm interference filter with a 17 nm fwhm band-pass (Schott). The emission photons were detected with a microchannel plate photomultiplier (Hamamatsu R1564U-01). The start signal was provided by a fast photodiode (Becker & Hickel: APM-400) detecting the second harmonic output of the laser. The single photon pulses from the detector were fed into a 1.6 GHz amplifier (Becker & Hickel: HFAC-26) which output is connected to the STOP input of the TCSPC computer card (Edinburgh Instruments TCC900). The instrument response function is 60 ps (fwhm). The signal was collected automatically by changing every 50 s the orientation of the emission polarizer in parallel or perpendicular orientation and back. The emission decay was stored in 2048 channels (24 ps/channel). Decays of EII^{mtl} mutants were corrected using equimolar concentrations of Trp-less EII^{mtl}.[26] The buffer was 20 mM Tris-HCl pH 8.4, 250 mM NaCl, 1 mM reduced gluthatione, and 0.25% $C_{10}E_5$ detergent at 20 °C. Excitation was at 305 nm. *p*-Terphenyl in ethanol was used as monoexponential deconvolution reference (τ = 1.08 ns). Data were analyzed with a model of discrete exponentials using the TRFA data processing package, version 1.2, of SSTC, Belarusian State University, Belarus.

Ionization Potential Measurements. The setup used for the multiphoton ionization photoelectron spectroscopy (MPI-PES) experiments is described in detail elsewhere.[43,44] Briefly, a laser pulse (0.1−1.0 mJ/pulse, 15 ns fwhm) from a dye laser is focused with a 25 mm quartz lens into an effusive beam of the sample. The photoelectrons formed by multiphoton ionization are parallelized by a strongly diverging magnetic field and detected after traveling through a 0.5 m flight tube. The time-of-flight spectrum is recorded on a digital oscilloscope and can be converted into a kinetic energy spectrum after transfer to a computer.

In previous studies ionization potentials have been determined using dispersed photoelectron spectroscopy (PES) in which a retarding voltage on the flight tube is increased in a stepwise fashion and only the high-resolution part of the time-of-flight (TOF) spectrum is converted into the energy domain. To avoid complications by accidental resonances at intermediate levels and photodissociation processes, it turned out that for the present study it was more useful to employ a two-dimensional photoelectron spectroscopy (2D-PES) approach in which the laser is scanned stepwise and at every wavelength the entire averaged TOF spectrum (typically for 100 laser shots) is written to a file. From these 2D-PES images ionization thresholds can be determined straightforwardly as well, albeit with a slightly worse resolution than with dispersed PES.

Results

Ionization Potentials. Table 1 shows B3LYP DFT-calculated adiabatic IPs for a selection of 20 substituted benzenes and indoles using two basis sets, 6-31G* and 6-311+G(2df,2p), and also shows experimental values, including seven shown in bold

(33) Wayland, E.; Noland, C. R. *J. Org. Chem.* **1967**, *32*, 828−832.
(34) *Gaussian 98*, revision A.11.3; Gaussian, Inc.: Pittsburgh, PA, 2002.
(35) Lee, C.; Yang, W.; Parr, R. G. *Phys. Rev. B* **1988**, *37*, 785.
(36) Wetmore, S. D.; Boyd, R. J.; Eriksson, L. A. *Chem. Phys. Lett.* **2000**, *322*, 129−135.
(37) *MOLCAS5.4*, version 5.4; Lund University: Sweden, 2000.
(38) Pierloot, K.; Dumez, B.; Widmark, P.-O.; Roos, B. O. *Theor. Chim. Acta* **1995**, *90*, 87.
(39) Ridley, J.; Zerner, M. *Theor. Chim. Acta (Berl.)* **1973**, *32*, 111.
(40) Nishimoto, K.; Mataga, N. *Z. Phys. Chem. (Frankfurt)* **1957**, *13*, 140.
(41) Li, J.; Williams, B.; Cramer, C. J.; Truhlar, D. G. *J. Phys. Chem.* **1999**, *110*, 724−733.
(42) Callis, P. R. *Int. J. Quantum. Chem.* **1984**, *S18*, 579−588.
(43) Rijkenberg, R. A.; Buma, W. J.; van Walree, C. A.; Jenneskens, L. W. *J. Phys. Chem. A* **2002**, *106* (21), 5249−5262.
(44) Rijs, A. M.; Backus, E. H. G.; de Lange, C. A.; Westwood, N. P. C.; Janssen, M. H. M. *Electron Spectrosc. Relat. Phenom.* **2000**, *112*, 151.

Table 1. Calculated and Experimental Ionization Potentials (IPs) (eV) of 20 Compounds

name	B3LYP/ 6-31G*	B3LYP/ 6-311 +G(2df, 2p)	experimental IP	predicted IP[a]
benzene	8.787	9.062	9.244[45]	9.256
fluorobenzene	8.709	9.016	9.20[46]	9.210
methylbenzene (toluene)	8.353	8.594	8.828[47]	8.788
5-fluoroindole	7.47	7.793	**7.975** ± 0.008[b]	7.986
7-fluoroindole	7.393	7.756		7.949
4-fluoroindole	7.341	7.697		7.891
2-fluoroindole	7.355	7.685		7.878
7-aza-3-methylindole	7.398	7.655		7.848
6-fluoroindole	7.328	7.653	**7.819** ± 0.008[b]	7.845
3-fluoroindole	7.295	7.633		7.827
indole	7.276	7.579	7.760[48], **7.765** ± 0.008[b]	7.771
5-fluoro-3-methylindole	7.212	7.511	**7.729** ± 0.009[b]	7.703
7-fluoro-3-methylindole	7.165	7.503		7.697
5-methylindole	7.158	7.449	7.6493[49], **7.651** ± 0.007[b]	7.643
4-fluoro-3-methylindole	7.097	7.418		7.611
6-fluoro-3-methylindole	7.112	7.413		7.607
2-fluoro-3-methylindole	7.111	7.416		7.609
1-methylindole	7.081	7.366	7.5319[49], **7.526** ± 0.012[b]	7.558
3-methylindole	7.041	7.321	**7.539** ± 0.010[b]	7.514
5-hydroxy-3-methylindole	6.849	7.166		7.357

[a] From linear regression of columns 3 and 4. [b] This work.

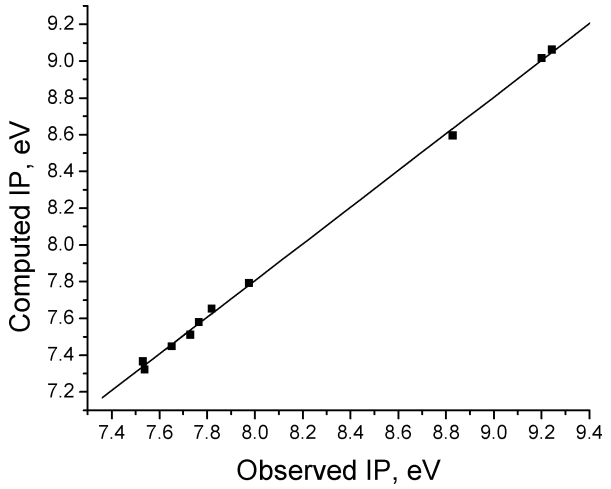

Figure 2. Plot of B3LYP/6-311+G(2fd,2p) computed IPs against observed values (points) and linear regression (line).

measured in this study after the computations were completed. No adjustments in the computations were made following the new measurements. Figure 2 shows the linear regression plot of the calculated (B3LYP/6-311+G(2df, 2p)) vs the experimental values. The standard deviation is 0.02 eV. The last column of Table 1 shows values predicted from the regression plot. In this study we focus on the differential effect of 5-fluoro and 6-fluoro substitution. From column 3 of Table 1 it is seen that the IP for 5F3MI is computed to be 0.190 eV higher than that for 3MI and the measured difference is 0.190 ± 0.019 eV. If the predicted difference is taken from the regression line, the difference is 0.189 eV. For 5FI the computed difference is 0.214, again in excellent agreement with the experimental difference 0.210 ± 0.02 eV. Corresponding results using 6-31G* were within 0.03 eV of these numbers.

The calculated IP difference between 6FI and indole is 0.074 eV, while the measured value is 0.054 ± 0.01 eV. More pertinent is the calculated IP for 6F3MI, which is 0.092 eV higher than that of 3MI. In the absence of an experimental value for 6F3MI, we use 0.09 ± 0.02 eV for this difference.

Adding fluoro is seen to increase the IP for all indoles, but substitution at the 5 position is the most effective, followed closely by the 7 position. From the 6FI results, one expects the IP of 6FTrp to be at least 0.1 eV lower than that of 5FTrp.

Zero-Point Energies. Upon ionization, all C−H stretching frequencies increase, and almost all skeletal vibrational frequencies decrease for both benzenes and indoles. This is due to removal of an electron from the predominantly π bonding highest occupied molecular orbital (HOMO). For benzenes, the skeletal modes dominate and there is a net decrease in zero-point energy (ZPE) upon ionization. However, for the indoles the balance is much closer, with the C−H and N−H stretches often dominating slightly. Including ZPE corrections for the indoles in this work modifies the predicted change in IP by fluoro substitution by only about 0.01 eV.

Effect of Solvent on Spectra. In Figure 3 the UV absorption and fluorescence spectra for 5FNATA and NATA are presented in five different solvent systems. In all solvents the absorption and emission spectra of 5FNATA are red-shifted compared to the spectra of NATA. In buffer, the shift in absorbance is 7 ± 1 nm or 0.1 ± 0.01 eV. These spectra indicate that the excitation-induced permanent dipole changes in NATA and 5FNATA are comparable for the emitting state.

Fluorescence Anisotropy. Excitation anisotropy spectra were recorded for NATA and 5FNATA to further characterize the effect of 5-fluoro substitution on the photophysics of NATA. These are shown in Figure 4. 5F3MI was included to confirm the results obtained for 5FNATA. The results for NATA are essentially the same as those reported in an earlier study.[50] The dip in intrinsic anisotropy (A_0) is at 290 nm, the wavelength of the $S_0-{}^1L_b$ origin.[51] The A_0 emission wavelength dependence of NATA has not been reported before but shows, as expected, only a slight dependency, indicative for one emitting S_1 state (Figure 4B). Except in apolar solvents, the emitting state of NATA is known to be ${}^1L_a$.[52] Comparable excitation anisotropy spectra were obtained for 5FNATA and 5F3MI. The dip in A_0 is 7 nm red-shifted to 297 nm, and no large emission wavelength-dependence of A_0 is observed. This, together with the results presented in Figure 3, confirms that ${}^1L_a$ is the emitting state of 5FNATA. Deconvolution of the excitation-anisotropy spectra of 5FNATA and 5F3MI (Figure 4) into the ${}^1L_a$ and ${}^1L_b$ spectra, using the same approach as that in ref 50, shows that, as for Trp, the ${}^1L_a$ and ${}^1L_b$ bands overlap in 5FTrp (data not shown). In fact, the red-shift in absorbance onset of 5FTrp is predominantly caused by the shift in ${}^1L_b$, which has an intense, narrow origin band, and that is more sensitive to 5-substitution than is ${}^1L_a$.[50] Emission is from ${}^1L_a$, regardless of which state is initially excited because of fast (<1 ps) internal conversion and environment relaxation about the large ${}^1L_a$ dipole.[53] The larger dipole also means the ${}^1L_a$ origin is much broader than that of ${}^1L_b$, causing the absorption at the longest wavelengths to be dominated by ${}^1L_a$. The A_0 of 5FNATA at 310 nm is 0.27. 5F3MI

(45) Nemeth, G. I.; Selzle, H. L.; Schlag, E. W. *Chem. Phys. Lett.* **1993**, *215* (1−3), 151−155.
(46) Fujisawa, S.; Ohno, K.; Masuda, S.; Harada, Y. *J. Am. Chem. Soc.* **1986**, *108* (21), 6505−6511.
(47) Lu, K. T.; Eiden, G. C.; Weisshaar, J. C. *J. Phys. Chem.* **1992**, *96* (24), 9742−9748.
(48) Hager, J. W.; Wallace, S. C. *Anal. Chem.* **1988**, *60*, 5−10.
(49) Lin, L. L.; Zhang, S.; Tzeng, W. B. *J. Chem. Phys.* **2004**, *120*, 5057−5063.
(50) Eftink, M. R.; Selvidge, L. A.; Callis, P. R.; Rehms, A. A. *J. Phys. Chem.* **1990**, *94* (9), 3469−3479.
(51) Valeur, B.; Weber, G. *Photochem. Photobiol.* **1977**, *25*, 441−444.
(52) Callis, P. R. *Methods Enzymol.* **1997**, *278*, 113−150.
(53) Shen, X. H.; Knutson, J. R. *J. Phys. Chem. B* **2001**, *105* (26), 6260−6265.

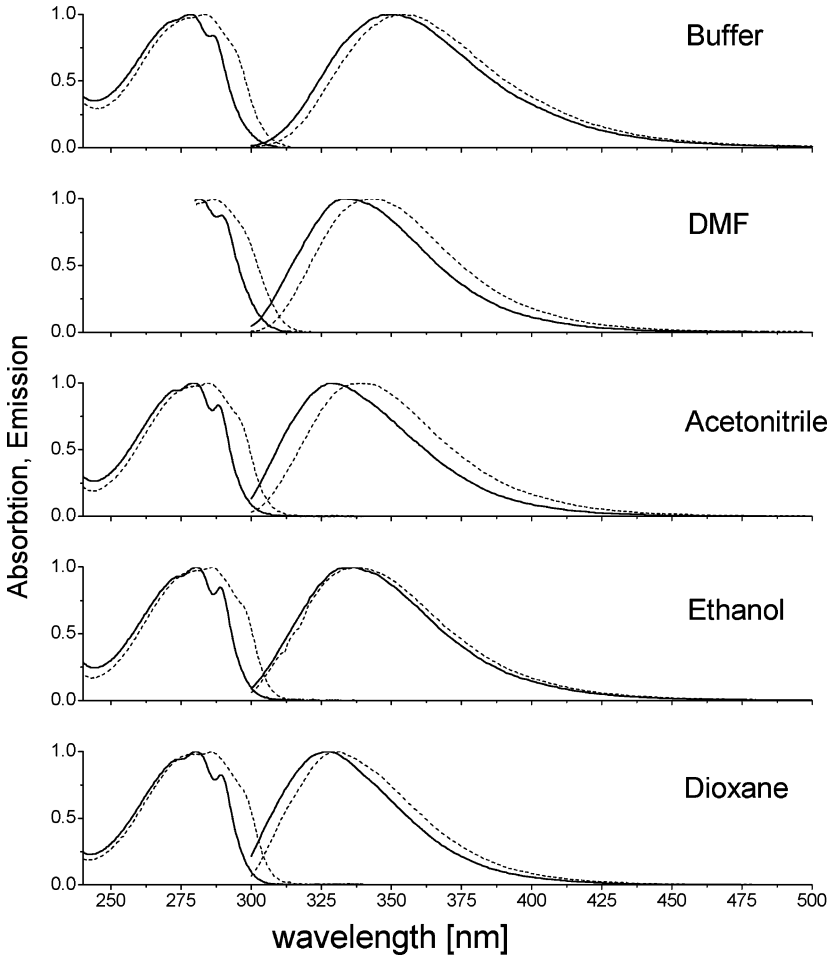

Figure 3. Solvent dependence of absorption and fluorescence for NATA (solid lines) and 5FNATA (dashed lines) in 10 mM TrisHCl pH = 7.4, DMF, acetonitrile, ethanol, and dioxane at room temperature. All spectra were normalized. The extinction coefficients at maximum absorbance in buffer are the same for Trp and 5FTrp.[55]

absorbs more strongly than 5FNATA > 310 nm, and a limiting A_0 of 0.29 was found at 314 nm.

Effect of Fluoro Substitution in Indole from CASPT2 Calculations. Table 2 compares the result of CASPT2 and ZINDO calculations of the vertical excitation energies to the ^1L_a and ^1L_b states for indole and 3MI to their 5- and 6-fluoro counterparts. ZINDO results are included here for comparison because of their predictive value in QM-MM simulations of the ^1L_a fluorescence wavelength[54] and ET quenching.[23,24] In rows 7−12 the same is done for two different sandwich complexes of indole and formamide. Both have an interplanar separation of 4.5 Å. Complex (1) has the formamide directly over the indole, and in complex (2) the formamide is displaced by a few Å (see Supporting Information for coordinates and images). For the complexes, the vertical excitation energy to the lowest indole−amide charge transfer (CT) states is shown. In every case, both ^1L_a and ^1L_b transitions are shifted a few nm to lower energy by 5-fluoro substitution, consistent with conclusions reached from our spectroscopic experiments seen in Figures 3 and 4. 6-Fluoro substitution appears to cause almost no shift within the accuracy of these calculations. The CASPT2-computed CT−^1L_a energy gap is shifted to higher energy by 2500−2900 cm^{-1} (0.29−0.34 eV) for the 5FI complex and by 1100−2500 cm^{-1} (0.14−0.31 eV) for the 6FI complex, results consistent with the increased IPs and decreased ^1L_a excitation energies for the indole ring found in this work. We note that in our experience the differences in vertical transition energies track closely to the more pertinent adiabatic differences.

Figure 5 summarizes the results of the IP calculations and spectroscopic information that predict a 0.29 eV (2340 cm^{-1}) increase in ΔG_0 for 5FTrp. Also shown are the HOMO and LUMO of 3MI and 5F3MI obtained from B3LYP/6-311+G-(2df,2p) calculations, showing the great similarity of corresponding MOs in the two systems. The figure is something of a caricature because the $S_1(^1L_a)$ transition energies are not exactly the difference in the MO energies and Koopman's theorem is not exactly obeyed. The three lines in the center depict three amide CT states corresponding to three (for example) supposed conformations whose environments and donor−acceptor distances could give rise to different CT energies. The energy separations are unknown at present. They could be large enough to completely account for all lifetime heterogeneity at one extreme or essentially zero at the extreme wherein the lifetime heterogeneity is entirely determined by electronic coupling heterogeneity (see Discussion section).

Fluorescence Lifetimes for 6FTrp in Proteins. As noted above, 6-fluoro substitution is predicted to increase the IP of Trp by about 0.09 eV. 6FTrp is commercially available, and the impact of its smaller IP increase on the lifetime heterogeneity was investigated by incorporating 6FTrp into three single-Trp

(54) Vivian, J. T.; Callis, P. R. *Biophys. J.* **2001**, *80*, 2093−2109.

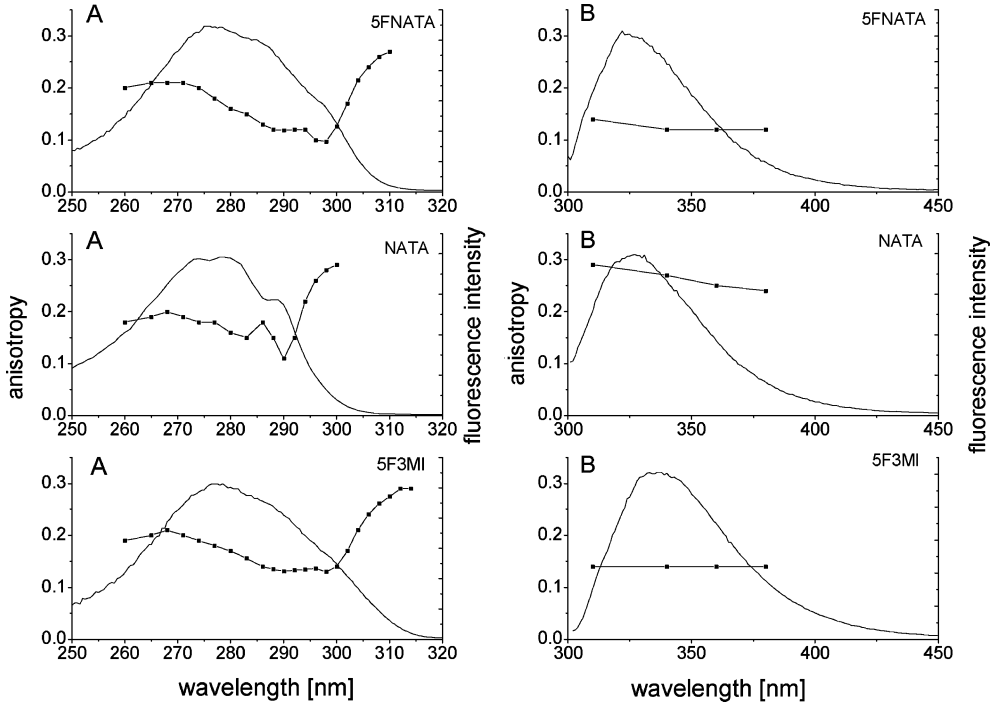

Figure 4. Fluorescent properties of 5FNATA, NATA, and 5F3MI in PG glasses at −55 °C. (A) Excitation spectra and excitation anisotropy values (■). The emission was collected at 360 nm. (B) Emission spectra and the emission-wavelength-dependence of the anisotropy upon excitation at 295 nm (■).

Table 2. CASPT2 and ZINDO Calculations of Vertical ^1L_a, ^1L_b, and CT Transition Energies (in kilo cm^{-1}) Showing the Effect of 5- and 6-Fluoro Substitution for Indoles and Indole Amide Complexes

	caspt2			zindo		
	L_a	L_b	CT	L_a	L_b	CT
indole	38.25	34.76		37.44	33.43	
5-fluoroindole	37.99	34.14		36.95	32.91	
6-fluoroindole	38.32	34.69		37.01	33.02	
3-methylindole (3MI)	37.08	34.35		36.73	33.2	
5-fluoro-3MI	36.83	33.81		36.35	32.75	
6-fluoro-3MI	37.14	34.60		36.50	32.98	
indole-formamide (1)	39.04	32.43	68.56	38.91	34.28	61.63
indole-formamide (2)	38.93	32.42	72.08	38.84	34.27	64.42
5-fluoroindole-formamide[a] (1)	38.88	31.54	71.27	38.49	33.73	64.35
5-fluoroindole-formamide (2)	38.76	31.54	74.42	38.42	33.73	67.38
6-fluoroindole-formamide (1)	37.94	32.19	70.00	38.22	33.85	62.98
6-fluoroindole-formamide (2)	38.63	32.20	72.90	38.15	33.84	66.28

[a] The geometry for the fluoroindole-containing complexes is identical to the corresponding indole sandwich except for the bond to the fluorine.

mutants of EII^{mtl}, harboring a Trp at position 30, 42, or 117 (mutants W30, W42, and W117, respectively). The lifetimes of these mutants containing Trp have been reported before.[26] The isolation procedure has been significantly changed since, and therefore these proteins have been isolated and analyzed anew, following the same procedures as those for the Trp-analog-containing proteins. Lifetime data for all three modifications are now presented on an equal footing in Table 3. The decay for each Trp-containing protein has three lifetimes, and fitting of the data with 4 exponentials did not further improve the fit. The decay for the 6FTrp-containing proteins shows only two lifetimes, one of 3−4 ns and one of 7−9 ns. A longer average lifetime of 6FTrp, compared to Trp, in proteins has been reported before.[55] These data indicate that an increase in the CT−^1L_a energy gap of ∼0.09 eV measurably reduces lifetime heterogeneity but does not virtually eliminate it, as in the case of 5FTrp. The emission maxima of 6FTrp in the five solvents of Figure 3 are all red-shifted compared to NATA (on average 9 nm, data not shown), indicating that also for this Trp analogue the emitting state is ^1L_a and that upon excitation the dipole moment changes similarly to what is observed in Trp.

(55) Wong, C.-Y.; Eftink, M. R. *Biochemistry* **1998**, *37*, 8938−8946.

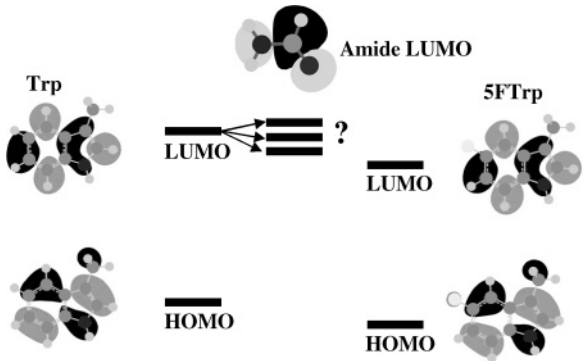

Figure 5. Symbolic representation of the effect of 5-fluoro substitution on the ionization potential, excitation energy, and molecular orbitals (MOs) of Trp. The putative acceptor amide MO is shown with postulated discrete charge-transfer energy levels for different structural subpopulations.

Table 3. Fluorescence Decay Parameters of Single-Trp EII^{mtl} Mutants W30, W42, and W117 Containing Trp, 6FTrp, or 5FTrp[a]

	Tau1 [ns] (α)	Tau2 [ns] (α)	Tau3 [ns] (α)	Tau avg [ns]	χ^2
W30-Trp	1.0 (0.34)	2.9 (0.64)	5.6 (0.02)	2.3	1.07
W30-6Ftrp	4.4 (0.74)	7.3 (0.26)		5.2	1.29
W30-5FFtrp	4.4				1.15
W42-Trp	1.7 (0.12)	4.0 (0.37)	6.4 (0.51)	4.9	1.07
W42-6FTrp	3.3 (0.38)	8.2 (0.62)		6.3	1.09
W42-5FTrp	4.7				1.30
W117-Trp	1.8 (0.32)	3.7 (0.47)	6.6 (0.21)	3.7	1.12
W117-6Ftrp	3.6 (0.36)	9.1 (0.64)		7.1	1.15
W117-5FTrp	5.2				1.19

[a] The total intensity was assumed as $I(t) = \sum_i \alpha_i \exp(-t/\tau_i)$, $\sum \alpha_i = 1.0$. [b] Maximum number of counts/channel of each decay was 22 000−35 000.

Although 6-fluoro substitution causes no significant shift in the absorption spectrum, the red-shifts in the fluorescence indicate that 0.1 eV ± 0.05 eV should be added to the CT−^1L_a energy gap. The solvent shifts indicate that the 6FTrp results are in line with simulations addressing the impact of 6-fluoro substitution on the lifetime heterogeneity of Trp, as presented in the Discussion section.

Discussion

Nature of the Emitting State. That the emitting state (S_1) for 5FTrp in proteins is ^1L_a with virtually identical character to that of Trp is easily established from the similarity of emission solvent dependence and the excitation polarization spectra of NATA and 5FNATA (Figures 3 and 4). The independence of the intrinsic anisotropy on the emission wavelength further supports this (Figure 4B). The emission maxima of 5FTrp containing EII^{mtl} mutants is red-shifted by about 7 nm compared to the Trp-containing protein. A similar shift has been observed for 5FTrp versus Trp-containing mutants of Staphylococcal nuclease.[55] The computational results presented in this paper for 5FTrp are consistent with ^1L_a as the emitting state. Similarly, one may conclude that ^1L_a is also the emitting state for 6FTrp, since the fluorescence emission shows a comparable solvent dependence as found for NATA and 5FNATA. If the emitting state were ^1L_b, the fluorescence maximum is expected to be only minimally sensitive to changes in the microenvironment, as is observed, for example, for 5OHTrp.[56−58]

Nonexponential Decay Is Not from Spectral Relaxation. Because of the great similarity of the fluorescence wavelength sensitivity of Trp and 5FTrp, the nonexponential fluorescence decay observed for Trp in the EII^{mtl} mutant proteins cannot arise because of a time-dependent shift of the fluorescence spectrum, as has been strongly advocated[11] and plausibly demonstrated in some cases.[59] The nearly identical solvent dependence means that the permanent dipole change upon excitation of 5FTrp is of the same order as that for Trp and would be therefore equally capable of driving relaxation.

Electron-Transfer Rate Heterogeneity. Below we discuss two potent, but distinctly different, sources of heterogeneity that could cause nonexponential fluorescence decay. In the context of ET rate constants (k_{ET}), these are termed energy gap heterogeneity and interaction heterogeneity. As noted in the Introduction, there is ample reason to believe that the sensitivity to environment, and therefore also lifetime heterogeneity, for Trp protein fluorescence comes mostly from intrinsic ET quenching wherein an electron is transferred from the indole ring to a nearby amide of the peptide backbone.[17−22] We will contend that the positioning of the CT state energy is nearly optimal for such sensitivity, being sufficiently high in energy that typical variations in structure and/or electrostatics are sufficient to modulate this ET rate over the range from being noncompetitive with other S_1 depopulation channels to being dominant. A useful form for the ET rate constant in the nonadiabatic limit coming from Fermi's golden rule[60] is

$$k_{ET} = 4\pi^2 c V^2 \langle \rho_{FC} \rangle \quad (1)$$

(here with all energies expressed as wavenumbers, cm^{-1}). c is the speed of light, V is the quantum mechanical electronic coupling matrix element ("interaction") connecting the initial fluorescing state with the CT state. $\langle \rho_{FC} \rangle$ is the density of final vibronic states averaged over the separation in 0−0 transitions, ΔE_{00}, the energy difference for the removal of an electron from the donor (indole ring) and the capture of an electron by the acceptor (amide), and is given by

$$\langle \rho_{FC} \rangle = (2\pi\sigma^2)^{-1/2} \int \rho_{FC}(\Delta E_{00}) \exp -{}^1/_2(\Delta E_{00} - \langle \Delta E_{00} \rangle / \sigma)^2 \, d\Delta E_{00} \quad (2)$$

σ is the standard deviation of the fluctuation of ΔE_{00} about its mean, $\langle \Delta E_{00} \rangle$.

The form in eq 1 is precisely the starting point for the well-known equation for *Förster resonance energy transfer* (FRET) rate, with the only difference being that ρ_{FC} comes from the overlap integral of the photoelectron spectra of donor and acceptor radicals instead of from the overlap of the fluorescence and absorption spectra of donor and acceptor, a parallel that has been noted previously.[60,61]

The widely used high-temperature classical limit equation for k_{ET} that has become almost synonymous with Marcus theory is displayed in eq 3.

$$k_{ET} = \left(\frac{4\pi^2}{h}\right) V^2 (4\pi\lambda k_B T)^{-1/2} \exp\left(-\frac{(\Delta G_0 + \lambda)^2}{4\pi\lambda k_B T}\right) \quad (3)$$

The connection between eqs 1−2 and eq 3 is traced from the first quantum mechanical treatment of nonadiabatic electron transfer by Levich and Dogonadze[62] through forms that recognize electron transfer as a case of radiationless electronic transition[63] (see extensive reviews by Marcus and Sutin,[64] Bixon and Jortner,[60] and Tachiya and co-workers[65]). In eq 3, λ is the reorganization energy, k_B is the Boltzmann constant, and ΔG_0 is the difference in free energy of the fluorescing and CT *equilibrium* states. The amplitude of the fluctuations in ΔE_{00} determines the width of the Gaussian and is related to the reorganization energy by $\sigma^2 = 2\lambda k_B T$. The average CT−$^1L_a$ energy gap is closely related to $\Delta G_0 + \lambda$.

Energy Gap Heterogeneity. In the case of FRET, ρ_{FC} is not usually written as an explicit function of ΔE_{00} because the distribution of ΔE_{00} is fairly narrow, and the variation with time for individual molecular pairs is not large. For ET, however, ΔE_{00} varies enormously in time because of the large CT state dipole and fluctuating electric fields in polar environments. Therefore, so too will ρ_{FC}, thereby providing one source of ET rate heterogeneity, e.g., in proteins. Because it is relatively small, this type of heterogeneity has almost never been a factor in discussions of FRET (except obliquely in reference to the Weber

(56) Ross, J. B. A.; Szabo, A. G.; Hogue, C. W. V. *Methods Enzymol.* **1997**, *278*, 151.
(57) Das, K.; Ashby, K. D.; Smirnov, A. V.; Reinach, F. C.; Petrich, J. W.; Farah, C. S. *Photochem. Photobiol.* **1999**, *70* (5), 719−730.
(58) Wong, C.-Y.; Eftink, M. R. *Protein Sci.* **1997**, *6*, 689−697.
(59) Toptygin, D.; Savtchenko, R. S.; Meadow, N. D.; Brand, L. *J. Phys. Chem. B* **2001**, *105*, 2043−2055.
(60) Bixon, M.; Jortner, J. *Adv. Chem. Phys.* **1999**, *106*, 35−202.
(61) Hopfield, J. J. *Proc. Natl. Acad. Sci., U.S.A.* **1974**, *71*, 3640−3644.
(62) Levich, V. G.; Dogonadze, R. R. *Dokl. Akad. Nauk SSSR, Ser. Fiz. Khim.* **1959**, *124*, 123−126.
(63) Kestner, N. R.; Logan, J.; Jortner, J. *J. Phys. Chem.* **1974**, *78*, 2148−2166.
(64) Marcus, R. A.; Sutin, N. *Biochim. Biophys. Acta* **1985**, *811*, 265−322.
(65) Barzykin, A. V.; Frantsuzov, P. A.; Seki, K.; Tachiya, M. *Adv. Chem. Phys.* **2002**, *123*, 511−616.

red edge effect[66]), but a strong case for its importance in ET has recently been made from QM-MM simulations of Trp in proteins.[23,24]

Interaction Heterogeneity. Another source of ET rate heterogeneity could, in principle, come from V. This is certainly true for FRET, where V is usually well approximated by the interaction of the donor and acceptor transition dipoles in the point-dipole approximation, so that V^2 depends on the inverse sixth power of the donor−acceptor distance and on the relative orientation of the transition dipoles. In ET theory, V^2 also varies strongly with both distance and donor−acceptor orientation,[67] depending approximately on the square of the overlap integral of the donor and acceptor MOs. For typical overlaps, V^2 decreases exponentially with D−A separation, providing that the relative orientation is fixed.[60] However, because of the multinodal properties of the MOs involved in typical cases, V^2 (the through-space part) is even more sensitive to relative orientation than FRET.[67] This type of heterogeneity has been the primary basis for explanations of nonexponential fluorescence decay for systems undergoing FRET quenching in nondiffusing systems.[12,68,69] Also it has played a central role in discussions of ET quenching-induced nonexponential fluorescence decay in which *only* the exponential distance dependence has been considered.[9,70,71]

Interaction Heterogeneity Cannot Alone Be Responsible. 5-Fluoro substitution cannot plausibly reduce V sufficiently to eliminate ET in the 5FTrp proteins considered here for the simple reason that both experimental and theoretical observations show that ^1L_a is the donor state. The differences between the ^1L_a state wave functions of 5FTrp and Trp are small. Assuming that the structure of the 5FTrp mutants is essentially the same as that for Trp, this means that V must be the same for the 5FTrp and Trp counterparts. The remaining viable mechanism is that 5-fluoro substitution increases ΔE_{00} sufficiently to effectively reduce the Franck−Condon overlap. ΔE_{00} depends on both the IP of the indole ring and on the ^1L_a energy in its lowest vibrational level. The IP values computed in this work show that ΔE_{00} is increased by 0.19 eV for 5FTrp due to the increased IP, and the red-shifted spectra add another 0.1 eV. Thus the CT state will be raised relative to ^1L_a by an average of 0.29 eV (2340 cm^{-1}), which, as we will see below, is an amount sufficient to reduce the ET rate in most cases to a negligible value. Similarly, for 6FTrp the increase in IP of ∼0.09 eV and the average fluorescence red-shift of 0.10 eV lead to an increased energy gap of ∼0.19 eV, which is sufficient to reduce, but not eliminate, lifetime heterogeneity. However, because the interaction and overlap are multiplied in the expression for the rate, it is not yet clear whether the range of lifetime heterogeneity observed with Trp can be explained by energy gap heterogeneity alone; if the interaction magnitude and the energy gap values are correlated, the interaction would provide amplification of the heterogeneity.

(66) Weber, G.; Shinitzky, M. *Proc. Natl. Acad. Sci. U.S.A.* **1970**, *65* (4), 823−830.
(67) Zhang, L. Y.; Friesner, R. A.; Murphy, R. B. *J. Chem. Phys.* **1997**, *107* (2), 450−459.
(68) Blumen, A.; Manz, J. *J. Chem. Phys.* **1979**, *71* (11), 4694−4702.
(69) Klafter, J.; Shlesinger, M. F. *Proc. Nat. Acad. Sci. U.S.A.* **1986**, *83* (4), 848−851.
(70) Adams, P. D.; Chen, Y.; Ma, K.; Zagorski, M. G.; Sonnichsen, F. D.; McLaughlin, M. L.; Barkley, M. D. *J. Am. Chem. Soc.* **2002**, *124*, 9278−9286.
(71) Yang, H.; Luo, G.; Karnchanaphanurach, P.; Louie, T.-M.; Rech, I.; Cova, S.; Xun, L.; Xie, X. S. *Science* **2003**, *302*, 262−266.

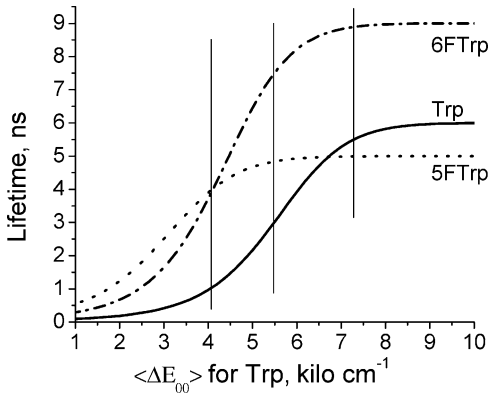

Figure 6. Multiple lifetimes from a pure energy gap heterogeneity model predicted using eqs 1 and 2 for ET rates with $\sigma = 2300$ cm^{-1} and $V = 25$ cm^{-1}, and using nonelectron-transfer decay rates typical of Trp (solid), 5FTrp (dotted), and 6FTrp (dash−dot). Vertical lines indicate the CT−^1L_a energy gaps assumed for Trp to give lifetimes of 1.0, 3.0, and 5.5 ns. The curves for 6FTrp and 5FTrp are displaced 0.19 and 0.29 eV (1530 and 2340 cm^{-1}), showing the effect of larger energy gaps.

Is 0.3 eV Sufficient? It is important at this point to ask whether a ∼0.3 eV shift in ^1L_a−CT energy gap can reasonably create the loss of ET quenching and lifetime heterogeneity observed. Figure 6 models the pure energy gap heterogeneity limit by displaying the calculated fluorescence lifetimes for Trp, 5FTrp, and 6FTrp as a function of average energy gap *for Trp* as given by eqs 1 and 2 with $\sigma = 2300$ cm^{-1} and $V = 25$ cm^{-1}. The lifetimes, τ, are calculated from $\tau = (k_0 + k_{ET})^{-1}$ where k_0 is the decay rate in the absence of ET and k_{ET} is the ET rate from eqs 1 and 2. k_0 values are representative of the long-lifetime components in Table 3. The curves for 5FTrp (dotted) and 6FTrp (dash−dot) are translated left by 2340 and 1530 cm^{-1} (0.29 and 0.19 eV), respectively, the amount of their respective fluoro-induced increased energy gap. The vertical lines are positioned to represent hypothetical energy gaps associated with subpopulations. They cross the Trp curve at 1.0, 3.0, and 5.5 ns, typical lifetimes for Trp in proteins. For 5FTrp, all three lifetimes merge into what is likely an unresolvable group, whereas, for 6FTrp, two lifetimes are predicted, one at ∼3.5 ns and two near 8 ns that would not typically be resolvable.

The parameter values used to achieve this degree of agreement with experiment are similar to those used in the global fit of calculated vs observed quantum yields by Callis and Liu for 24 selected Trps in 17 proteins ($V = 10$ cm^{-1} and $\sigma = 2300 \pm 1000$ cm^{-1}).[24]

It is also possible to model the effect of 5- and 6-fluoro substitution in the extreme of assuming that the lifetime heterogeneity arises only from subpopulations with different V. Figure 7 shows the same plot as that for Trp in Figure 6 for three different values of V, again with $\sigma = 2300$ cm^{-1}. At $\langle \Delta E_{00} \rangle = 6000$ cm^{-1} these three V values give lifetimes of 1.0, 3.0, and 5.5 ns, the intersections of the leftmost vertical line and characteristic of Trp. An increase of IP by 0.29 eV (representing 5FTrp) is indicated by the rightmost line. It is seen that this increase reduces the ET rates so that all three lifetime components lie between 5 and 6 ns, predicting a reduction from 3 to 1 component, assuming these are now not resolvable. Similarly, an increase of 0.19 eV (denoted by the middle vertical line), the value expected for 6FTrp, predicts a reduction of lifetime components from 3 to 2.

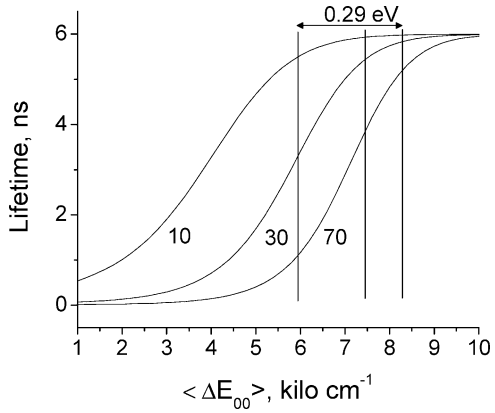

Figure 7. Multiple lifetimes predicted from a pure interaction heterogeneity model using eqs 1 and 2 for ET rates with $\sigma = 2300$ cm^{-1} and $V = 10$, 30, and 70 cm^{-1}, and using nonelectron-transfer decay rates typical of Trp. The vertical lines indicate the constant $\langle \Delta E_{00} \rangle$ values assumed for Trp, 6FTrp (displaced higher by 0.19 eV), and 5FTrp (displaced by 0.29 eV).

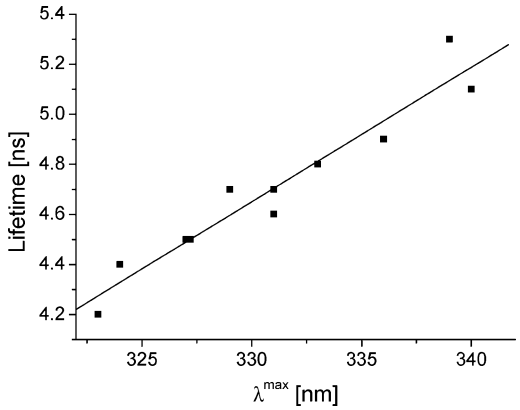

Figure 8. Relationship of the emission maximun (λ^{max}) of single-5FTrp-containing EII^{mtl} mutants to their monoexponential fluorescence lifetime. 5Ftrp was incorporated at positions 30, 32, 36, 42, 97, 114, 117, 126, 133, 188, and 327, all located in the membrane-embedded C domain of EII^{mtl}. Variation in 5FTrp lifetime from batch to batch is typically 0.1 ns.

The above exercise is only intended to draw attention to the type of information that may be accessed after more experiments are done on more proteins.[72] The astonishing effectiveness of the ~0.3 eV gap increase, however, appears to be roughly consistent with energy gap distributions and interactions inferred from simulations.[23,24]

To experimentally demonstrate that ~0.3 eV is sufficient to remove *all* lifetime heterogeneity for Trp in proteins depends on the ability of the analysis routines to resolve different lifetime components from the decay data.[73] For proteins exhibiting nonexponential decay wherein one of the components is extremely short, e.g., ~0.1 ns, analysis of the type shown in Figures 6 and 7 suggests that 0.3 eV will not generally be sufficient to eliminate ET and, therefore, that the 5FTrp fluorescence decay will be biexponential. This may be relevant to the observation of EII^{mtl} mutant 5FTrp109, which resides next to a cysteine, and which exhibits a biexponential decay.[25]

Significance. Regardless of the cause of lifetime heterogeneity and average lifetime variations between proteins, this work forces the realization that the $^1L_a-CT$ energy gap for Trp in proteins is optimally positioned so that small changes in gap will make a significant impact on the ET rate and, therefore, on lifetime and quantum yield. The usefulness of the sensitivity of Trp fluorescence intensity for monitoring protein structural changes depends on this optimal gap. If heterogeneity in protein structure exists for a particular protein, this will carry a high liability for lifetime heterogeneity. Conversely, probes such as 5FTrp, whose energy gap is too large to enable ET in most proteins, will not show much variation in quantum yield and lifetime in different protein environments.[25] They will not be useful for monitoring protein structural changes, e.g., folding/unfolding, but they will be much more useful for monitoring fluorophore-quencher proximity by Förster quenching[74] or by extremely potent quenchers, e.g., acrylamide, because there will not be the interfering background of lifetime heterogeneity from sources that are difficult to assign. Figure 8 demonstrates one impact of eliminating ET in 5FTrp. In general, a plot of Trp fluorescence lifetime in single-Trp-containing proteins vs wavelength of fluorescence shows no correlation.[2] In contrast, Figure 8 shows that lifetime and wavelength of currently available 5FTrp-containing mutants are well correlated and in a manner very close to that observed by Meech *et al.*[75] for 3MI in different solvents, where ET is not an issue.

Generality. The emphasis of this paper is on lifetime heterogeneity that is specifically exposed by controlling the average lifetime, apparently by controlling the ET quenching rate. There are many possible types of structural variation in proteins that can modulate the ET rate; these include solvent and protein hydrogen bond arrangement, relative positions of charged groups, and relative donor−acceptor geometry. Potentially all of these variables are affected by local (rotameric) and global protein conformation changes. In addition, most of these same mechanisms contribute to an *ET-independent* source of nonexponential decay caused by spectral relaxation.[11] Given sufficient time resolution (<1 ps), a wavelength-dependent nonexponential decay will be evident for almost all proteins because of rapid shifting of the fluorescence spectrum due to protein and solvent response to the greatly changed electronic charge distribution in the ^1L_a state.[52,53,76] This latter type of lifetime heterogeneity is largely obscured when a wide band of fluorescence wavelengths is observed and the time resolution is ≫1 ps, but at least one well documented case has been reported.[59] One value of the 5FTrp probe is that the relaxation time heterogeneity is expected to be virtually the same as that for Trp, thereby permitting a clear view of the ET-based heterogeneity.

Because the observations of monoexponential decay from 5FTrp have been to this point reported only for a rather restricted set of proteins, we cannot yet be certain that our conclusions are general. However, the extent of Trp lifetime heterogeneity is large, and the fluorescence wavelength maxima of the dozen

(72) The truth is unlikely to lie at the extremes depicted in the above cartoons. It is unreasonable to expect that $\langle \Delta E_{00} \rangle$ ($\Delta G_0 + \lambda$ in terms of eq 3) and σ could be the same for different structural subpopulations, given the strength of electrostatic interactions in proteins. It is also probably unreasonable to expect the ET rate to be independent of donor−acceptor distance. It is likely that the effect of V and $\Delta G_0 + \lambda$ are not separable.[78] In addition, V is likely to be quite orientation dependent,[67] further confounding attempts to correlate distance and lifetime.

(73) For example, analysis of the decays of 5FTrp-containing proteins (Table 3) while fixing a second component indicate that a 50% shorter lifetime with a 10% amplitude will remain unnoticed.

(74) Broos, J.; Pas, H. H.; Robillard, G. T. *J. Am. Chem. Soc.* **2002**, *124* (24), 6812−6813.

(75) Meech, S. R.; Lee, A.; Phillips, D. *Chem. Phys.* **1983**, *80*, 317−328.

(76) Pal, S. K.; Peon, J.; Bagchi, B.; Zewail, A. H. *J. Phys. Chem. B* **2002**, *106* (48), 12376−12395.

single-5Trp mutants of EII^{mtl} that show monoexponential decay span the range of 323 to 339 nm (Figure 8).

A. Other Modified Trps. Examination of the IP and emitting state excitation energies of other modified Trps should help to further clarify the factors contributing to nonexponential decay. To date, no other biosynthetically incorporable Trp analogue has been found to show monoexponential decay in proteins of the size studied in this work. Free 1-methyl-7-azaTrp decays monoexponentially, and this analogue has been chemically introduced into an octapeptide in which it also decays with one exponent.[4] When the octapeptide was bound to an antibody, however, the 1-methyl-7-azaTrp fluorescence decay was nonexponential.[4] The increased energy gap due to red-shifted spectra has previously been postulated by Petrich and co-workers to account for monoexponential decay through elimination of ET quenching for 7-AzaTrp.[77] The computed IP increase for 7-Aza3MI from Table 3 is 0.33 eV, even larger than that for 5F3MI, suggesting that the energy gap for 7-AzaTrp may be particularly large.

As already noted above, 6F3MI has a predicted IP that is about 0.09 eV lower than that of 5F3MI, and even this modest change markedly reduces the extent of lifetime heterogeneity. In constrast, 5-methyltryptophan (5MTrp) would be expected to show greater lifetime heterogeneity than Trp, because experiments and theory both show that 5MI has a *lower* IP by about 0.12 eV than that of indole. The utility of this modification hinges on whether 5-methyl substitution in Trp will change the nature of the fluorescing state from ^1L_a to ^1L_b.[50]

Conclusion and Future Work

The work reported here greatly strengthens the case that Trp fluorescence lifetime heterogeneity (nonexponential decay) and the large variation of average lifetimes between Trps in different protein environments are almost entirely due to the sensitivity of fluorescence quenching by electron transfer to local structure.

The experiments and calculations reported here show that 5-fluoro substitution increases the ionization potential of 3-methylindole by 0.19 eV. When combined with spectroscopic information, the energy change for electron transfer from the indole ring is therefore expected to increase by about 0.29 eV for 5FTrp relative to Trp, an amount that is sufficient to drastically reduce lifetime heterogeneity from structural substates having different electron transfer rates. The great similarity of the fluorescing state electronic structure for 5FTrp and Trp rules out the possibility that 5-fluoro substitution diminishes the electron interaction matrix element responsible for electron transfer and also rules out the possibility that nonexponential decay has its sole source in the relaxation of the fluorescence spectrum on a ns time scale. A subtle point is that the present information cannot discern the relative contributions of energy gap and interaction heterogeneity to lifetime heterogeneity. However, shutting off electron transfer solely with an energy shift means that lifetime heterogeneity is unlikely to arise from distance dependence of interaction *alone*, as is sometimes proposed.[9,70] Distinguishing between energy-gap and interaction-based rate heterogeneity may be possible with extensive studies using 5-methyltryptophan, whose IP is predicted to be smaller than Trp, and with other fluorinated Trps, whose IPs are predicted to be intermediate between those of Trp and 5FTrp.

The above conclusions lead to the realization that, independent of the fluorescent probe, monoexponential fluorescence decay and environment-sensitive fluorescence intensity are mutually exclusive properties in proteins whenever the lifetime is primarily controlled by electron-transfer quenching.

Acknowledgment. This work was supported by NSF Grant MCB-0133064 and the Netherlands Foundation for Chemical Research (SON) with financial aid from the Netherlands Organization for the Advancement of Scientific Research (NWO). P.R.C. and T.L. thank Prof. Andrzej Sobolewski for assistance in the early stages of our CASPT2 calculations.

Supporting Information Available: Cartesian coordinates and graphical views of indole−formamide sandwich complexes in Table 2. This material is available free of charge via the Internet at http://pubs.acs.org.

JA043154D

(77) Chen, Y.; Gai, F.; Petrich, J. W. *J. Phys. Chem.* **1994**, *98* (8), 2203−2209.
(78) Newton, M. D. *Theor. Chem. Acc.* **2003**, *110* (5), 307−321.